Am J Physiol Heart Circ Physiol 282: H1081–H1091, 2002;
10.1152/ajpheart.00498.2001.

Load dependence of ventricular performance explained by model of calcium-myofilament interactions

JUICHIRO SHIMIZU, KOJI TODAKA, AND DANIEL BURKHOFF
Division of Circulatory Physiology, College of Physicians and Surgeons, Columbia University, New York, New York 10032

Received 8 June 2001; accepted in final form 5 November 2001

Shimizu, Juichiro, Koji Todaka, and Daniel Burkhoff. Load dependence of ventricular performance explained by model of calcium-myofilament interactions. *Am J Physiol Heart Circ Physiol* 282: H1081–H1091, 2002; 10.1152/ajpheart.00498.2001.—Although a simple concept of load-independent behavior of the intact heart evolved from early studies of isolated, intact blood-perfused hearts, more recent studies showed that, as in isolated muscle, the mode of contraction (isovolumic vs. ejection) impacts on end-systolic elastance. The purpose of the present study was to test whether a four-state model of myofilament interactions with length-dependent rate constants could explain the complex contractile behavior of the intact, ejecting heart. Studies were performed in isolated, blood-perfused canine hearts with intracellular calcium transients measured by macroinjected aequorin. Measured calcium transients were used as the driving function for the model, and length-dependent rate constants yielding the highest concordance between measured and model-predicted midwall stress at different isovolumic volumes were determined. These length-dependent rate constants successfully predicted contractile behavior on ejecting contractions. This, along with additional model analysis, suggests that length-dependent changes in calcium binding affinity may not be an important factor contributing to load-dependent contractile performance in the intact heart under physiological conditions.

left ventricle; calcium transient; four-state model; excitation-contraction coupling

ALTHOUGH MANY EARLY STUDIES of isolated cardiac muscle showed a complex dependence of myocardial contractile force on length, rate, and extent of shortening, a simpler concept of load-independent behavior of the intact heart initially evolved from studies in isolated, intact blood-perfused hearts. These studies led to widespread acceptance of the end-systolic pressure-volume relationship (ESPVR) as a load-independent index of ventricular contractile state (29). Although the ESPVR approach has proven invaluable as a tool to quantify and track changes in ventricular contractile state under a wide range of conditions and has enabled new understanding of ventricular-vascular coupling, it is a phenomenological description of ventricular properties with no link to basic mechanisms of myofilament contraction. Additionally, it has become increasingly clear that loading conditions can influence the ESPVR (6, 7, 15).

Attempting to establish a link between the growing understanding of the biochemical interactions involved in muscle contraction and whole organ properties, we demonstrated the feasibility of a four-state biochemical scheme of calcium, actin, and myosin interactions (Fig. 1) to explain the complex contractile behavior of the intact heart under isovolumic conditions at different volumes (3, 5). Initial modeling studies led to experiments focused on characterizing length dependence of myocardial calcium sensitivity in intact hearts (28). We identified important quantitative differences in calcium sensitivity and load dependence of calcium sensitivity between intact hearts and isolated, superfused cardiac muscle (28). Our prior investigations, however, were limited to experiments performed under isovolumic conditions.

In the present study, calcium and ventricular pressure transients were measured on isovolumic and ejecting contractions in isolated, blood-perfused, physiologically afterloaded canine hearts. Using these data, we tested the hypothesis that the four-state model (Fig. 1) with length-dependent rate constants could explain contractile behavior of the intact, ejecting heart. Length dependence of rate constant values was determined from the isovolumic beats, and these were then used to successfully predict contractile performance on ejecting beats. The characteristics of intracellular calcium transients ($[Ca^{2+}]_i$) measured during abrupt changes in loading conditions challenged the notion that myofilament calcium binding is length dependent. Model analysis further showed that length-dependent calcium binding was not required for the model to accurately predict ventricular behavior over a wide range of loading conditions.

METHODS

Surgical Preparation

Six isolated, blood-perfused canine hearts were studied with standard techniques (32). A balloon connected to a volume servo-pump system secured inside the left ventricu-

Address for reprint requests and other correspondence: J. Shimizu, Dept. of Cardiovascular Physiology, Okayama Univ. Graduate School of Medicine and Dentistry, 2-5-1 Shikatacho, Okayama, 700-8558 Japan.

The costs of publication of this article were defrayed in part by the payment of page charges. The article must therefore be hereby marked "*advertisement*" in accordance with 18 U.S.C. Section 1734 solely to indicate this fact.

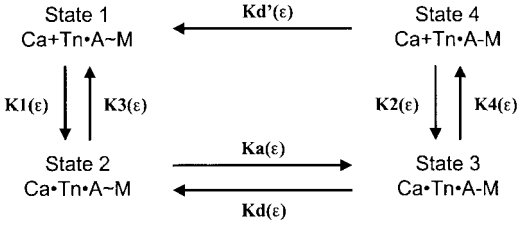

Fig. 1. Schematic representation of biochemical models proposed to account for interactions between calcium and myofilament and force generation. Tn, calcium-binding subunit of troponin; A, actin; M, myosin; ε, strain; K_1–K_4, rate constants for respective chemical reaction; K_a, association constant (actin-myosin affinity); K_d, dissociation constant for *state 3*; $K_{d'}$, dissociation constant for *state 4*.

lar (LV) chamber of the isolated heart was used to measure and control LV volume. A micromanometer (Millar) placed inside the balloon measured LV pressure (LVP). The volume servo system was commanded by a computer-generated windkessel impedance afterload (30, 31), which enabled investigation of ventricular properties under both physiologically ejecting and isovolumic conditions. Pacing electrodes were sutured to the apex of the LV, and the heart was paced at 120 beats/min. Coronary arterial pressure was fixed at ~80 mmHg by a servo system. The temperature of the perfusate was maintained at ~37°C by a heat exchanger so that the heart temperature was ~35°C. Physiological signals were digitized at a rate of 1 kHz and analyzed off-line.

Measurements of Calcium Transients

Aequorin injections were performed in the inferoapical region. Injections consisted of 3–5 μl of an aequorin solution (composition in mmol/l: 154 NaCl, 5.4 KCl, 1 $MgCl_2$, 12 HEPES, 11 glucose, and 0.1 EDTA with 1 mg/ml aequorin, adjusted to pH 7.40). Approximately six injections per heart were made just under the epimysium with a low-resistance glass micropipette with an inner diameter of ~30 μm (32). The surface of a photomultiplier tube (9235QA, Thorn EMI, Fairfield, NJ; energized by a Thorn EMI PM28R power supply set at 900 V) was positioned so that it was in contact with the aequorin injection region. The isolated heart and photomultiplier tube were positioned inside a lighttight box. Aequorin signals were calibrated into absolute $[Ca^{2+}]_i$ by perfusing the heart at the end of the experiment with a 50 mM calcium-5% Triton X-100 solution, which lyses the cells and exposes the remaining aequorin to high amounts of calcium (20, 28, 32). Luminescence signals of interest were normalized by the total light emission, L_{max}, estimated as the integral of the aequorin light signal collected from the point at which the signal was acquired to the end of the experiment multiplied by the rate constant for aequorin consumption (2.11/s; Ref. 20). The instantaneous L/L_{max} was then converted to time-varying $[Ca^{2+}]_i$ according to the following equation

$$\frac{L}{L_{max}} = \left(\frac{1 + K_r[Ca^{2+}]_i}{1 + K_{tr} + K_r[Ca^{2+}]_i}\right)^3 \quad (1)$$

where K_r and the rate constant for force recovery (K_{tr}) were as determined previously (20): $K_r = 4.5 \times 10^6$ mol^{-1}, $K_{tr} = 130$. Calcium signals were averaged and low-pass filtered to provide reasonably smooth transients. In a subset of studies we confirmed, with sonomicrometers implanted just under the epimysium, that the area into which aequorin was macroinjected shortened and lengthened normally during the cardiac cycle (in-fiber shortening fraction ranging between 12 and 16%).

Experimental Protocol

The protocol is illustrated in the original experimental recordings of Fig. 2. The volume servo system was set so that the LV ejected from a preload volume selected to provide an end-diastolic pressure of ~15 mmHg and against an afterload impedance adjusted to provide an initial ejection fraction of ~50%. After a steady state had been reached, the mode of contraction was switched to isovolumic at a preselected time during filling. The mode of contraction was then switched back to ejection with the original afterload settings, and the procedure was repeated between two and four times

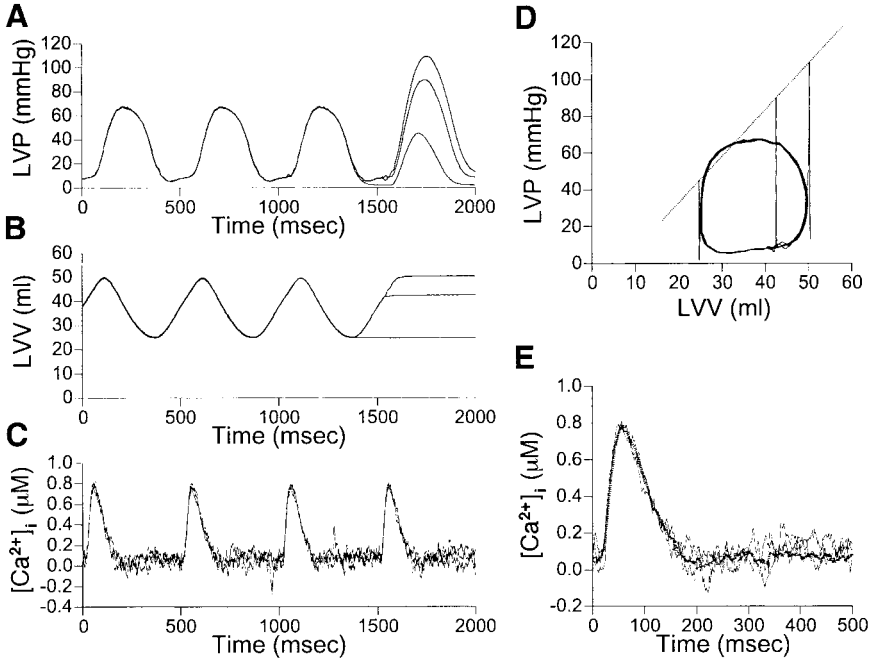

Fig. 2. Representative left ventricular (LV) pressure (LVP; *A*), volume (LVV; *B*), and calcium transients ($[Ca^{2+}]_i$; *C*) measured during steady-state ejecting contractions and on the first isovolumic beat of variously timed volume clamps. *D*: LVP-LVV loops corresponding to *A* and *B*. There is an approximately linear relationship between peak pressure and volume on the isovolumic contractions, and the pressure-volume loop of the ejecting beat "breaks through" this line. *E*: superimposed averaged $[Ca^{2+}]_i$ during steady-state ejecting contractions (dotted line) and during isovolumic contractions at the 3 different volumes; there is no detectable difference between these tracings.

at different isovolumic clamping volumes so that isovolumic data were obtained at three to five different volumes.

Calculation of Strain and Stress from Observed LV Volume and Pressure

To relate events measured in the ventricle to phenomena predicted by the biochemical model, LVP and ventricular volumes (LVV) were converted into myocardial stresses (σ; muscle force per unit cross-sectional area) and strains (ε; average normalized segment length) as described previously (12). For wall stress, the following equation was applied

$$\frac{\sigma_f}{P_{lv}} = 1 + 3\frac{V_{lv}}{V_w} \quad (2)$$

where P_{lv} is LV pressure, V_{lv} is LV cavity volume, and V_w is LV wall volume. For strain, the following equation was applied

$$\left(\frac{\varepsilon}{\varepsilon_{ref}}\right)^3 = \frac{V_{lv} + h \cdot V_w}{V_{lv,ref} + h \cdot V_w} \quad (3)$$

where ε is muscle strain, ε_{ref} is muscle strain at an arbitrarily defined reference state (we defined the reference state as the volume, $V_{lv,ref}$, at which end-diastolic pressure was 20 mmHg), and h is the fraction of the wall volume enclosed by the average layer. The fraction h was estimated to be 33% (12).

Determination of Load-Dependent Rate Constants

The measured calcium transients were used as the driving function for the simultaneous differential equations that describe the four-state biochemical model of contraction (detailed in the APPENDIX), and muscle stress [assumed to be proportional to the total number of strong actin-myosin bonds (A-M)] was the output

$$\sigma(t) = \alpha(\varepsilon)([Ca \cdot Tn \cdot A\text{-}M] + [Tn \cdot A\text{-}M]) \quad (4)$$

where α(ε) is proportional to the force generated by a single cross bridge as a function of strain (28). Myofilament cooperativity accounting for the fact that myofilament interactions are influenced by force generation, a factor previously shown to be critical for explaining contractile behavior, was also introduced into the model as summarized previously (4, 9, 25). Rate constant values were optimized (downhill simplex algorithm) to minimize the root mean squared (RMS) difference between predicted (σ_p) and measured (σ_m) stress at each strain: $RMS = (1/n)SQRT[\Sigma(\sigma_m - \sigma_p)^2]$ where n is the number of digitized points acquired during a given contraction. This procedure yielded strain-dependent rate constant values as detailed previously (3). These strain-dependent rate constants were then used in the four-state biochemical model to test whether stress on an ejecting beat could be predicted from the measured calcium transient and strain pattern.

Because it is controversial as to whether or not troponin C calcium binding affinity is length dependent, two different model analyses were performed. In *analysis 1*, all parameters of the model were allowed to vary with ventricular volume under the assumption that both calcium binding affinity of troponin and actin-myosin binding affinity vary with strain. In *analysis 2*, however, calcium-binding affinity of troponin was assumed to be independent of strain. In *analysis 2*, therefore, length dependence of myofilament performance lies solely in the cross-bridge interaction. For each analysis, the value of each rate constant was plotted as a function of strain. Results showed that there was always a reasonably linear relationship between parameter values and strain, so these were each summarized by linear regression.

Application of Four-State Model to Ejecting Contractions

To apply the four-state model to ejecting contractions, we made the following assumptions: *1*) the rate constants of the four-state model change instantaneously as a function of strain but are independent of the shortening velocity; and *2*) the force per unit cross bridge will change with shortening velocity according to Hill's equation (13). With these assumptions, generated stress on shortening contractions is described as follows

$$\sigma = \alpha(\varepsilon)([Ca \cdot Tn \cdot A\text{-}M] + [Tn \cdot A\text{-}M]) \quad \left(\frac{d\varepsilon}{dt} \geq 0\right) \quad (5)$$

$$\sigma = \frac{\alpha(\varepsilon)H_b - H_a\left|\frac{d\varepsilon}{dt}\right|}{\left|\frac{d\varepsilon}{dt}\right| + H_b}([Ca \cdot Tn \cdot A\text{-}M] + [Tn \cdot A\text{-}M]) \quad \left(\frac{d\varepsilon}{dt} < 0\right)$$

where α(ε) is the maximum force per unit cross bridge ($mmHg \cdot \mu mol^{-1} \cdot l^{-1}$), and H_a ($mmHg \cdot \mu mol^{-1} \cdot l^{-1}$) and H_b (s^{-1}) are constants of the Hill equation (13).

RESULTS

Intracellular Calcium Transients Are Not Significantly Different Between Ejecting and Isovolumic Contractions

Representative pressure and calcium transients measured during steady-state ejecting beats and on the first isovolumic beat of variously timed volume clamps are shown in Fig. 2. As shown in Fig. 2*D*, there is an approximately linear relationship (dotted line) between peak pressure and volume on the three isovolumic beats. The pressure-volume loop obtained on the ejecting beat "breaks through" that line, indicating an increased effective contractile state during ejection compared with isovolumic contractions as reported previously (6). Calcium transients from the final three ejecting beats and the first isovolumic contraction of these series are shown in Fig. 2*C*. Because the aequorin signals are bright, each signal shown was obtained by signal-averaging only two to four transients, which were obtained by repeating each loading sequence two to four times. In Fig. 2*E*, the calcium transient of the last ejecting beat is superimposed on the transients from each of the three isovolumic contractions. There was no detectable difference between these curves. Such data were obtained from all six hearts of this study and, as summarized in Table 1, neither peak calcium nor the duration of the calcium transient (measured at a value of 10% of the peak value) was influenced by the volume at which the clamp was imposed. Thus there is no detectable influence of volume or shortening on the calcium transient over a physiological range of volumes and ejection patterns despite the marked influence on pressure generation. As discussed in *Time course of calcium binding*, this finding implies that myofilament calcium binding affinity is not length dependent. This suggests

Table 1. *Influence of loading condition on characteristics of calcium transient*

Contraction Mode	Peak $[Ca^{2+}]_i$, μM	$[Ca^{2+}]_i$ Width, ms
Ejection	0.803 ± 0.270	180.2 ± 22.3
Isovolumic beat (ESV)	0.797 ± 0.310	180.5 ± 30.0
Isovolumic beat (Mid)	0.794 ± 0.269	186.4 ± 27.0
Isovolumic beat (EDV)	0.819 ± 0.305	174.3 ± 20.1

Values are means ± SD. $[Ca^{2+}]_i$, calcium transient; ESV, isovolumic contraction at the end-systolic volume of the ejecting beat; EDV, isovolumic contraction at the end-diastolic volume of the ejecting beat; Mid, isovolumic contraction at a volume between ESV and EDV of the ejecting beat.

that, for the four-state model, rate constants related to calcium binding (K_1–K_4) do not vary with muscle length or ventricular volume.

Four-State Model Predicts Stress on Isovolumic Contractions at Different Strains

The solid lines in Fig. 3 show the midwall myocardial stress transients estimated from the three isovolumic pressure waves of Fig. 2. With the measured calcium transients as the driving functions (Fig. 2*E*), the parameter values of the four-state model were optimized to provide the best concordance between the model predicted and the measured stress curves. As shown, the model is able to describe the stress transients very well at each strain with either *analysis 1* (dashed lines; calcium affinity of troponin allowed to vary with strain) or *analysis 2* (dotted lines; constant calcium affinity of troponin). Rate constant values as a function of strain for this example are shown in Fig. 4 for both analyses. Over the range of strains encountered, there was a reasonably linear relationship between each parameter value and strain. The RMS difference between the measured and predicted stress curves was determined for each of 39 isovolumic contractions examined in this study. The results showed that RMS was equally low for both *analysis 1* and *analysis 2* (1.8 ± 1.3 and 2.8 ± 0.7 mmHg, respectively), indicating, on a statistical basis, that both models provided good predictions of isovolumic stress curves. The average (±SD) values for all model parameter values obtained from all studies for both *analysis 1* and *analysis 2* are summarized in Table 2.

Ejecting Contractions

The solid lines in Fig. 5, *A*–*C*, show the measured calcium transient, midwall strain (ε), change in ε with time (dε/d*t*), and midwall stress, respectively, during the ejecting contraction corresponding to the isovolumic data shown in Fig. 3. The stress-strain loop is shown in Fig. 5*D*. With the measured calcium transient and strain curve as inputs and the strain-dependent parameter values for the four-state model determined under isovolumic conditions (Fig. 4), it is seen that both *analysis 1* (dashed lines) and *analysis 2* (dotted lines) predicted the stress measured during ejection well (Fig. 5, *C* and *D*). Values for H_a and H_b, the parameters that characterize the force-velocity relationship (*Eq. 5*), were adjusted to optimize the model prediction. Despite the difference in rate constants, the best fit values for H_a and H_b were not significantly different for *analyses 1* and *2* (H_a: 0.928 ± 0.263 vs. 0.943 ± 0.101 mmHg·μmol^{-1}·l^{-1} and H_b: 17.4 ± 6.14 vs. 17.7 ± 2.93 s^{-1}, respectively; n = 13 for each analysis). Thus the calculated instantaneous force per unit cross bridge during the contraction (Fig. 5*E*) showed a similar time course during the beat for the two analyses. This example and other examples shown in Fig. 6 are representatives of model predictions of 13 such ejecting contractions analyzed in this manner both at high and low ejection fractions. The RMS difference between measured and predicted stress curves on the ejecting beats was similar between *analysis 1* and *analysis 2* (1.7 ± 0.7 and 1.6 ± 0.7 mmHg, respectively), and each was smaller than obtained on the isovolumic contractions. Thus both models are equally good at prospectively predicting the stress curve under ejecting conditions from rate constant values obtained from isovolumic contractions.

Physiological Behavior of Four-State Model

To further test the validity of the four-state model, several basic physiological muscle properties were predicted and compared with experimental results from prior studies.

Myofilament calcium sensitivity. Myofilament calcium sensitivity is classically indexed by measuring the relationship between force (σ) and calcium concentration under steady state, equilibrium (nontwitch)

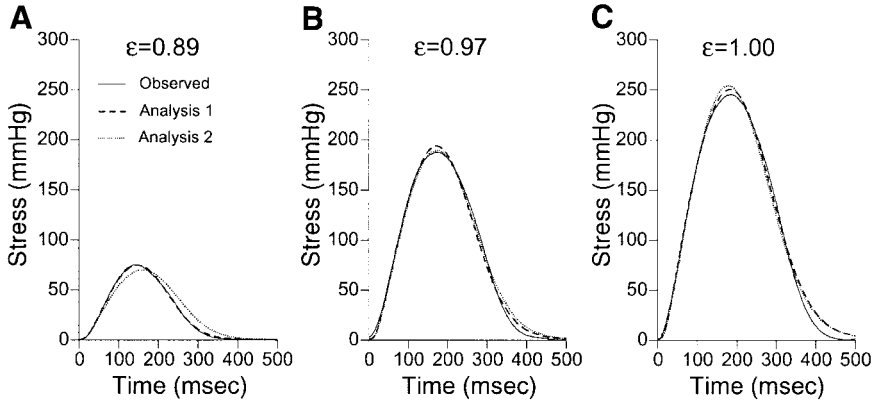

Fig. 3. Representative measured (solid lines) and model-predicted pressure curves of the first isovolumic contractions at different volumes after the same preceding steady-state ejecting conditions. Dashed lines are stress curves predicted by *analysis 1*, and dotted lines are stress curves predicted by *analysis 2*.

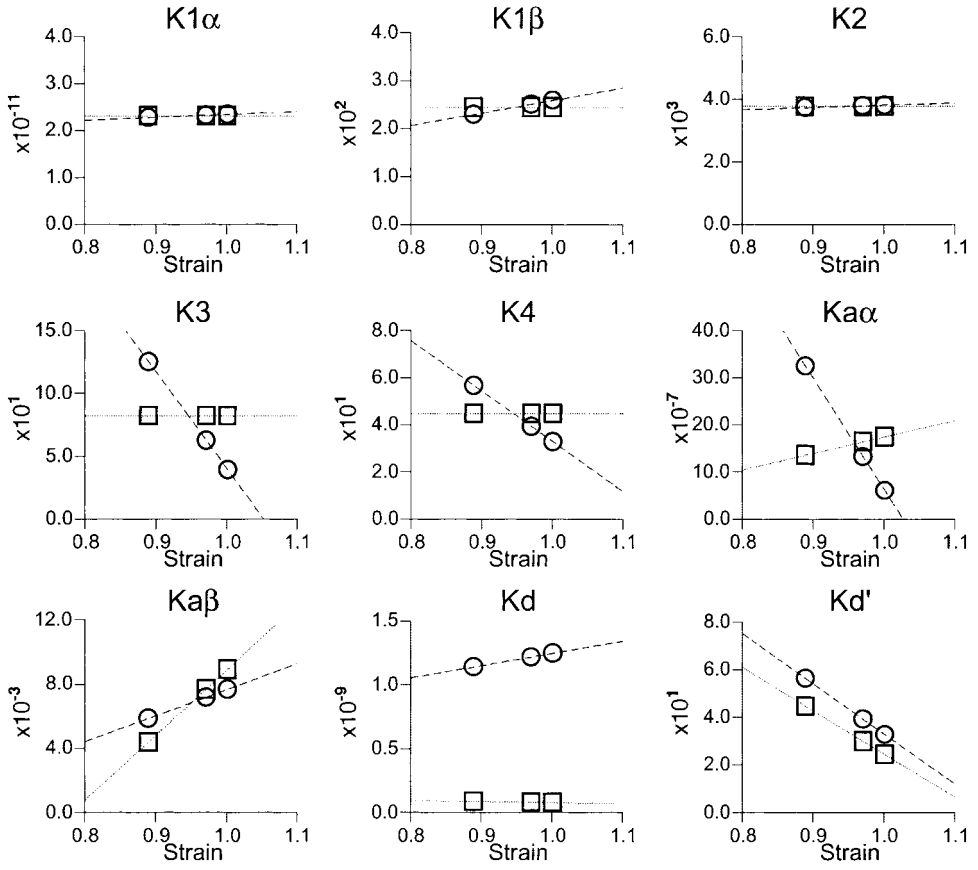

Fig. 4. Results from 1 representative heart showing how rate constant values vary as a function of strain. Dashed lines are for *analysis 1* and dotted lines are for *analysis 2*. Note that rate constants K_1–K_4 are constrained to be independent of strain in *analysis 2*.

conditions (force-pCa curves). This was simulated by imposing constant calcium concentrations on the four-state model. The resulting data provided typical sigmoidal curves (Fig. 7*A*, data from *analysis 2*), which were fit to Hill equations

$$\sigma = \frac{\sigma_{max}[Ca^{2+}]_i^{\eta_H}}{\{K_{1/2}^{\eta}[Ca^{2+}]_i^{\eta_H}} \quad (6)$$

where η_H is the Hill coefficient and $K_{1/2}$ is the calcium concentration for 50% maximal activation. $K_{1/2}$ decreased as strain increased, a consequence of the experimentally determined strain dependence of the rate constants. For strains varying between 1.00 and 0.92, $K_{1/2}$ values ranged between 0.061 and 0.123 μM. Hill coefficients averaged ~4, did not vary significantly

Table 2. *Mean parameter values obtained from analysis of all isovolumic contractions*

	Analysis 1		*Analysis 2*	
Rate Constant	Slope	Intercept	Slope	Intercept
$K_{1\alpha}$	1.49×10^{-7}	-1.07×10^{-7}	2.74×10^{-8}	
	$\pm3.03\times10^{-7}$	$\pm2.21\times10^{-7}$	$\pm5.23\times10^{-8}$	
$K_{1\beta}$	4.87×10^{2}	-2.13×10^{2}	2.36×10^{2}	
	$\pm4.94\times10^{2}$	$\pm4.25\times10^{2}$	$\pm1.09\times10^{2}$	
K_2	3.91×10^{2}	1.68×10^{3}	2.06×10^{3}	
	$\pm4.50\times10^{2}$	$\pm1.96\times10^{3}$	$\pm2.39\times10^{3}$	
K_3	-3.36×10^{2}	-3.56×10^{2}	3.74×10^{1}	
	$\pm3.13\times10^{2}$	$\pm3.33\times10^{2}$	$\pm3.49\times10^{1}$	
K_4	-1.14×10^{2}	1.41×10^{2}	3.26×10^{1}	
	$\pm1.16\times10^{2}$	$\pm1.25\times10^{2}$	$\pm1.34\times10^{1}$	
$K_{a\alpha}$	-1.25×10^{-5}	-1.39×10^{-5}	-2.34×10^{-6}	4.01×10^{-6}
	$\pm8.06\times10^{-6}$	$\pm7.72\times10^{-6}$	$\pm1.14\times10^{-5}$	$\pm1.17\times10^{-5}$
$K_{a\beta}$	1.92×10^{-2}	-1.24×10^{-2}	2.75×10^{-2}	-2.03×10^{-2}
	$\pm3.35\times10^{-3}$	$\pm3.67\times10^{-3}$	$\pm9.44\times10^{-3}$	$\pm8.20\times10^{-3}$
K_d	3.06×10^{-11}	1.80×10^{-9}	8.65×10^{-11}	1.13×10^{-8}
	$\pm1.01\times10^{-9}$	$\pm2.42\times10^{-9}$	$\pm1.28\times10^{-9}$	$\pm1.50\times10^{-8}$
$K_{d'}$	-7.91×10^{1}	1.10×10^{2}	-2.07×10^{2}	2.22×10^{2}
	$\pm1.66\times10^{2}$	$\pm1.68\times10^{2}$	$\pm5.71\times10^{1}$	$\pm4.57\times10^{1}$

Values are means ± SD; n = 13 in each analysis. $K_{1\alpha}$, $K_{1\beta}$, $K_{a\alpha}$, $K_{a\beta}$, adjustable constants. See Fig. 1 for definitions of K_1–K_4, K_d, and $K_{d'}$.

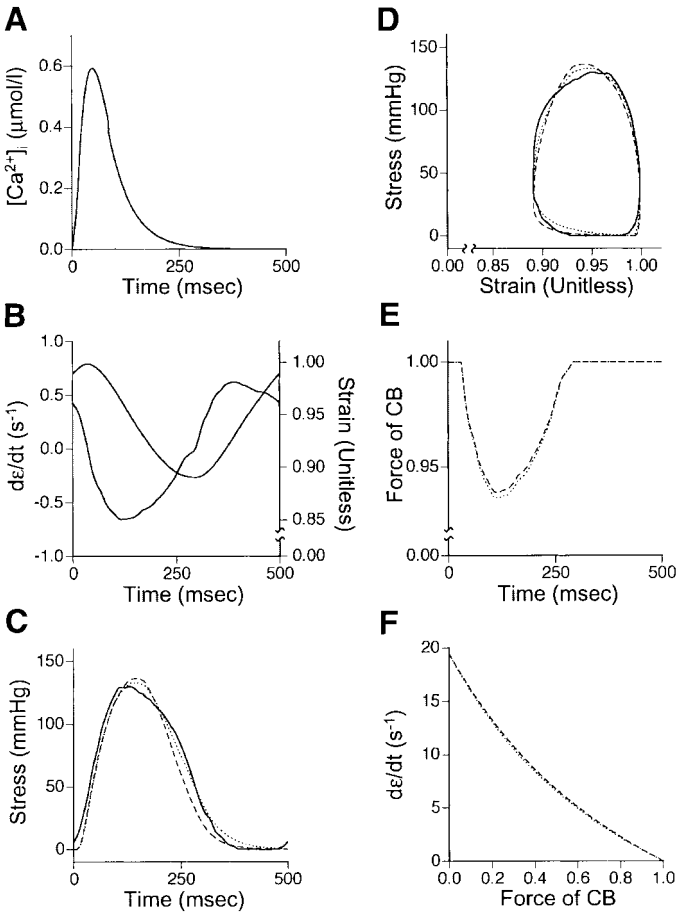

Fig. 5. *A*: representative calcium transient during steady-state ejecting contraction. *B*: midwall strain (ε) and change in ε with time (dε/d*t*). *C*: measured (solid line) and predicted midwall stress curves. *D*: measured (solid line) and predicted stress-strain loops corresponding to data in *B* and *C*. *E*: calculated instantaneous force per unit cross bridge (CB) during the ejecting contractions. *F*: predicted force-velocity relationship from *Eq. 3*. In each panel, the dashed line shows results from *analysis 1* and the dotted line shows results of *analysis 2*.

with strain, and did not vary significantly between *analysis 1* and *analysis 2* (Table 3).

Time course of calcium binding. It has been suggested that the amount of calcium bound to the myofilament varies as a function of length and that this contributes importantly to the Frank-Starling relationship (1). The amount of bound calcium as a function of time predicted by each analysis at three different strains is shown in Fig. 7, *B* and *C*. For *analysis 1* (Fig. 7*B*), where calcium binding rate constants K_1–K_4 are allowed to vary with strain, calcium binding increases with length. For *analysis 2* (Fig. 7*C*), with invariant calcium binding constants, calcium binding is similar for contractions at different lengths. This aspect of predicted muscle physiology fundamentally differentiates *analyses 1* and *2*.

Pressure-flow relationship. To determine how the model predicts that ejection velocity would impact on contractile performance we explored the relationship between ventricular flow and pressure at specific times during the contraction. Representative results are shown in Fig. 8. For each condition tested, strain patterns were set to achieve a common value (ε_s) at a common time (t_s). For example, in Fig. 8*A*, a family of strain curves is shown all of which start ejection 115 ms after the onset of contraction and achieve a strain of 0.990 at a time of 125 ms after the onset of contraction but start from different initial strains and therefore attain different ejection velocities at t_s. Model-predicted stress curves are shown in the graph. Similar curves are shown for ε_s values of 0.985 and 0.980 in Fig. 8, *B* and *C*, respectively. The stresses and strain rates were converted into LVP and flow rates, respectively, as described in METHODS. Pressure was then plotted as a function of flow, as shown in Fig. 8*D* for the data of Fig. 8, *A*–*C*. As shown, there is a negative, linear relationship between flow and pressure. Neither the slope of the relationship nor the flow-axis intercept (Q_{max}) varied with ε_s (indistinguishable results obtained with *analyses 1* and *2*). These simulated experiments were repeated for a common value of ε_s but for various values of t_s; a representative example is shown in Fig. 8*E* for an experiment with an ε_s value of 0.985. As shown again, the pressure-flow relation is linear with a negative slope that varies with t_s but with a relatively invariant Q_{max} value. For the parameter values obtained in the present study, Q_{max} values of ~800 ml/s were obtained, which is only slightly greater than the ~700 ml/s reported in the original studies of this phenomenon (27). All of the fundamental features of the pressure-flow relationships are thus reproduced by the four-state model.

Quick releases. Studies of isolated cardiac muscle have revealed that important insights into cross-bridge kinetics and calcium handling are obtained by studying how force responds to quick release-restretch loading sequences during steady-state contractures (4, 9). Such loading sequences were simulated at different calcium concentrations, and the time course of force redevelopment was analyzed. Figure 9, *A* and *B*, shows simulated force tracings during steady-state contractions at the specified calcium concentrations (0.1, 0.16, 0.25, and 1.0 μmol/l) and at a strain (ε = 1.0) for *analysis 2*. The rate constant (K_{tr}) of force recovery was determined and plotted as a function of calcium for each strain (Fig. 8*C*). As evidenced by the tracings, K_{tr} increased substantially with increased calcium concentration. There was little difference in predictions between *analyses 1* and *2*.

DISCUSSION

Hemodynamic loading conditions did not influence the macroinjected aequorin luminescence transient measured in blood-perfused intact hearts at 35°C over a physiological range of loads. We conclude from this, as discussed further below, that calcium binding is not strongly influenced by length under these conditions. It was further demonstrated that contractile behavior of the intact, ejecting heart can be predicted by a model of myofilament-calcium interactions in which calcium

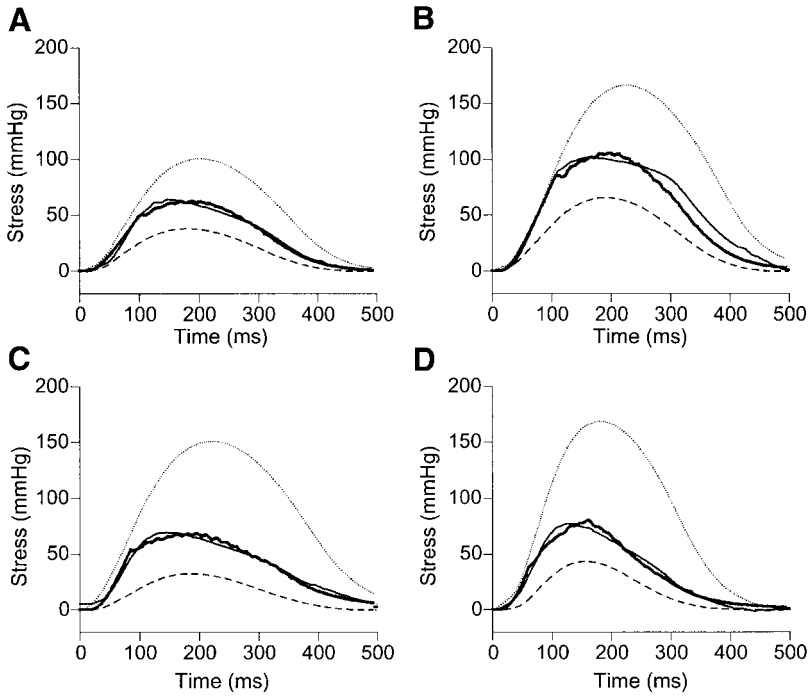

Fig. 6. Additional examples of measured (thin solid line) and prospectively predicted (by *analysis 2*; thick solid line) stress curves during ejecting contractions from model rate constant values determined under isovolumic contractions. The stress curves of isovolumic beats clamped at end-diastolic volume (dashed line) and at end-systolic volume (dotted line) are also shown. *A* and *B*: high ejection fractions (≈50%). C and *D*: low ejection fraction (~15%). Results obtained with *analysis 1* were indistinguishable.

binding is not influenced by length but other rate constants of myofilament interactions and their length dependence are determined under isovolumic conditions.

We showed in a prior study (32) with the same experimental methods that relatively small differences in calcium transients that paralleled changes in pressure development observed over longer time periods after a sustained change in loading conditions could be detected in isolated canine hearts with macroinjected aequorin luminescence measured from the epicardium. This is an important similarity to observations made originally by Allen and Kurihara (2) in isolated muscle. Aequorin luminescence is bright with this technique, requiring signal averaging of as few as two beats to obtain high-fidelity signals with low signal-to-noise ratios. Changes in strain during typical ejecting contractions in the epicardial layers from where the calcium transients are recorded are similar to those estimated for the midmyocardial layers. These factors render the methods used in the present study appropriate for studying changes in calcium kinetics under physiological conditions and would have detected these changes had they occurred.

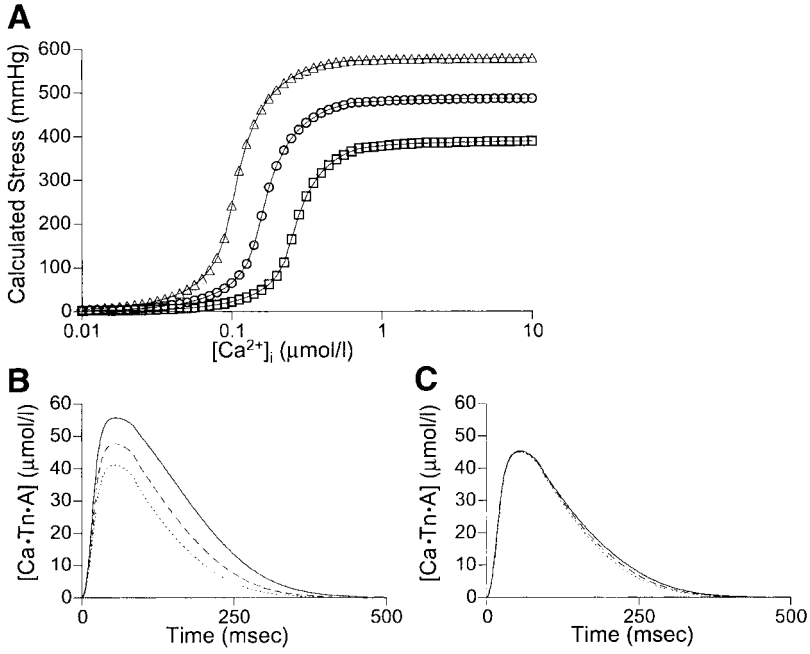

Fig. 7. *A*: representative force-calcium curves based on *analysis 2* at various strains (ε = 1.00, ○; 0.96, □; 0.92, △). These curves shifted leftward and upward with increasing strain. *B*: predicted time course of bound calcium (i.e., sum of amount of *state 2* and *state 3* of Fig. 1) for *analysis 1*, in which calcium binding rate constants (K_1–K_4) are allowed to vary with strain; calcium binding increases with length. *C*: for *analysis 2*, with length-independent calcium binding rate constants, bound calcium is similar for isovolumic contractions at different strains.

Table 3. *Parameters of sigmoidal Hill equation describing steady-state relationship between calcium and myofilament stress*

Strain ε	*Analysis 1*			*Analysis 2*		
	σ_{max}, mmHg	η_H	$K_{1/2}$, mmol/l	σ_{max}, mmHg	η_H	$K_{1/2}$, mmol/l
0.92	386.00 ± 24.03*†	3.724 ± 1.231	0.101 ± 0.036*	405.24 ± 37.33*†	4.080 ± 1.325	0.097 ± 0.024*
0.96	434.25 ± 22.23*†	3.881 ± 1.371	0.080 ± 0.032*	447.03 ± 29.50*†	4.027 ± 1.218	0.077 ± 0.022*
1.00	480.50 ± 22.04*†	3.943 ± 1.314	0.058 ± 0.028*	495.14 ± 23.81*†	3.975 ± 1.249	0.056 ± 0.021*

Values are means ± SD; $n = 13$. σ_{max}, η_H, Hill coefficient; $K_{1/2}$, $[Ca^{2+}]$ for 50% maximal activation. *$P < 0.05$ vs. $\varepsilon = 0.92$; †$P < 0.05$ vs. $\varepsilon = 0.96$.

Comparable results have been obtained in some studies of isolated, superfused papillary muscles in which peak intracellular calcium did not change significantly immediately after length changes (2, 14, 19, 21). Because it is estimated that ~95% of total released calcium is bound to the myofilament and calcium indicators (like aequorin) measure only free calcium, even small changes in myofilament affinity would be detected as substantial changes in free calcium.

In contrast, load-dependent changes in the rate of fall of free calcium have been noted in prior studies of isolated superfused muscles (2, 19). Such changes were not observed in the present study. Changes in the time course of the calcium transient were also not identified in a recent study of rat trabeculae (18). There are several possible reasons for such discrepancies. Differences in experimental conditions include blood perfusion vs. crystalloid superfusion (the latter potentially increasing cellular and interstitial water content), higher (more physiological) temperature in the intact heart, and influences of possible damage during the muscle isolation process. The findings in isolated muscles could thus reflect muscle behavior outside the boundaries of physiological conditions. Although the conditions under which isolated muscles are studied are more controllable and the measurements are less subject to artifacts and less devoid of confounding aspects of complex ventricular geometry and activation sequence than measurements in the intact heart, results obtained from intact hearts should not be dismissed on this basis.

In a study of crystalloid-perfused ferret hearts, our laboratory previously showed (3) that rate constants could be determined such that the four-state model with cooperativity (i.e., force-dependent actin-myosin binding affinity) was able to accurately fit isovolumic pressure curves from the measured calcium transient. With regard to isovolumic contractions, the present study extends these previous findings by showing how rate constants vary with volume and providing their values under the more physiological conditions of blood perfusion. On the basis of these values, model-predicted steady-state force-pCa curves were sigmoidal with η_H of ~4, similar to other studies of isolated muscle preparations and isolated heart preparations (1, 28). In prior studies, but not in the present study,

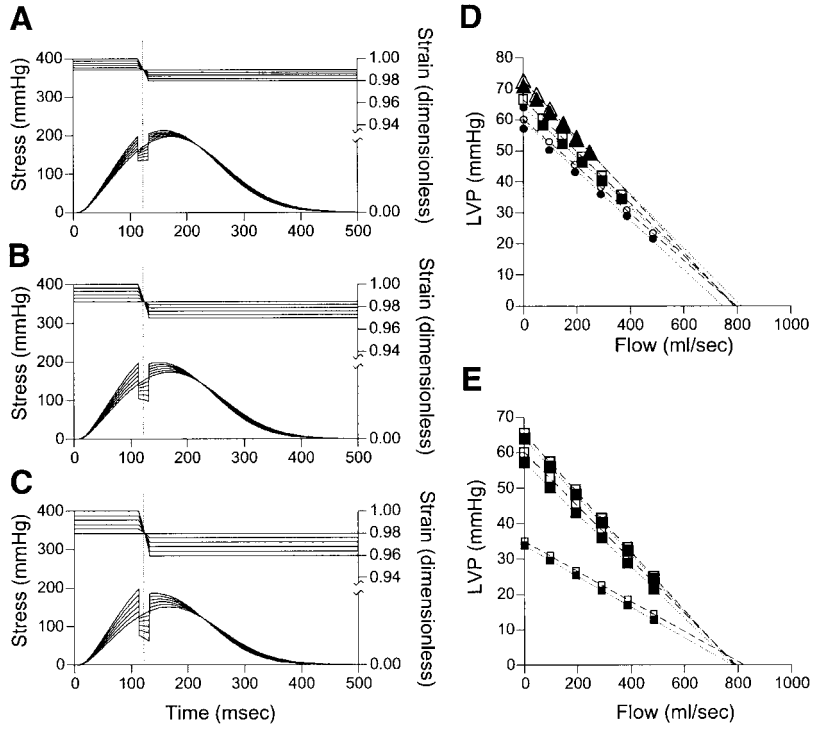

Fig. 8. Simulated stress responses to various shortening patterns designed to achieve specific strains (ε_s) and specific times (t_s) during a contraction to measure the ventricular pressure-flow relationship. *A–C*: representative simulations at $t_s = 125$ ms and $\varepsilon_s = 0.990$ (*A*), 0.985 (*B*), and 0.980 (*C*). Stress predicted by the model and $d\varepsilon/dt$ (s^{-1}) were transformed into LV pressure (LVP) and change in volume with time (dV/dt; ml/s), respectively. *D*: averaged results ($n = 13$) that represent effect of strain on Q_{max} (extrapolated *x*-axis intercept) at a constant t_s (125 ms). Q_{max} was approximately independent of ε_s (large symbols, $\varepsilon_s = 0.990$; middle-sized symbols, $\varepsilon_s = 0.985$; small symbols, $\varepsilon_s = 0.980$) at $t_s = 125$ ms ($P < 0.001$ by ANCOVA), and slopes of the relations are not significantly different. *Analysis 1* (open symbols and dashed lines) and *analysis 2* (closed symbols and dotted lines) have similar results in this simulation. *E*: averaged results that represent effect of t_s on Q_{max} at constant ε_s (0.985).

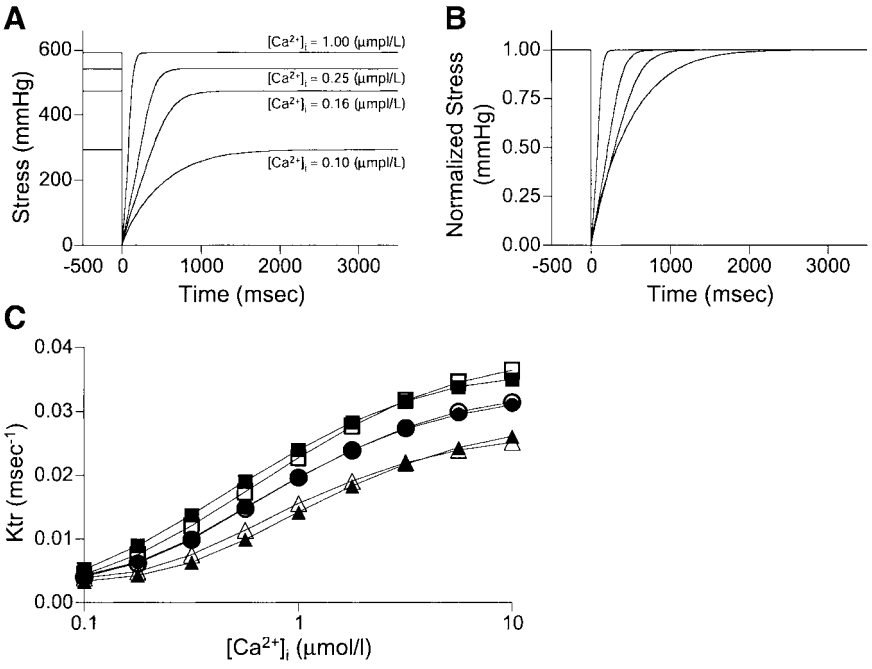

Fig. 9. Example of simulated force redevelopment after quick release and restretch during steady-state contracture at calcium concentrations of 0.10, 0.16, 0.25, and 1.00 μmol/l at a strain ε = 1.00. *A*: predicted stress curves. *B*: same force traces as in *A* with each normalized to its maximum to show more clearly changes in the time course of force redevelopment with calcium concentration. *C*: relationship between calcium concentration and rate constants of force redevelopment (K_{tr}). K_{tr} in *analysis 1* (filled symbols) and *analysis 2* (open symbols) show clear dependence on calcium concentration at each strain (ε = 1.00, squares; 0.96, circles; 0.92, triangles).

length-dependent increases in η_H have been observed. This includes one study from our own laboratory (28) in which η_H varied from 4.91 to 3.87 with strain values from 1.00 to 0.75. Differences in experimental factors noted above could have contributed to this relatively minor difference.

There is precedence for the notion that length dependence of myofilament activation can occur without length dependence of troponin C-calcium binding affinity, such as occurs in slow skeletal muscle (24). The overall force-calcium relationship is determined by both troponin C-calcium affinity and by actin-myosin interactions. Thus by influencing myofilament interaction kinetics (e.g., actin-myosin lattice spacing and binding affinities, the magnitude of cooperativity), length exerts its influence on force development. For example, the rate of force redevelopment (K_{tr}) reflects such intrinsic myofilament properties and the present results suggest a strong dependency of K_{tr} both on the level of myofilament calcium activation and on muscle (or sarcomere) length, as was shown experimentally in prior studies (23).

The application of the four-state model to ejecting contractions as implemented in the present study represents, to the best of our knowledge, the first attempt to model contractile behavior of ejecting contractions based on measured calcium transients with model parameter values obtained under isovolumic conditions. Prior theoretical studies have shown that one or another model could in general explain contractile behavior during shortening (17, 22), but there has been no prior attempt to explicitly test those models against measured data. The breadth of phenomena explained by the present model, however, should be acknowledged.

It could be argued that studies such as this should be performed in superfused isolated muscles. The use of epicardial calcium measurements from a single site and relating them to global pressure development presents several potential limitations. However, for reasons discussed above and specifically because certain key aspects of contractile behavior observed in intact hearts are not generally observed in isolated muscle, we considered it to be appropriate and important to investigate the phenomena under the more physiological conditions encountered in intact hearts. Results of several studies support the notion that, despite a seemingly complex ventricular geometry, myocardial activation sequence, and potential heterogeneity of muscle properties, conclusions pertaining to cellular and myofilament properties can be based on assessments of average midwall stresses and strains determined from intact hearts (8, 10, 11, 16, 26).

Additionally, there are a few limitations in converting LVV and LVP into strain and stress. First, strain calculated with this model does not necessarily equate with strain measured in a single sarcomere. Second, defining the reference point for strain (i.e., the point at which ε = 1) at an end-diastolic pressure of 20 mmHg does not necessarily equate to L_{max}, the preload that provides maximal sarcomere length of ~2.3 μm. Despite the potential lack of a strict 1:1 correspondence between calculated strain and true sarcomere length, use of midwall strain has proven over the years to be a useful means of quantifying changes in muscle stretch for purposes of comparing results from different hearts and for comparing results from intact hearts and isolated muscles and has been used in countless studies of ventricular mechanics. Furthermore, no claim of 1:1 correspondence between calculated strain and sarcomere length is required for any of the interpretations of the present study.

In conclusion, two important concepts have been revealed in the present study. First, measurements

with aequorin show that the intracellular free calcium transients are not influenced by abrupt changes in loading conditions, suggesting that myofilament calcium binding is not likely to be length dependent in vivo. Second, the four-state model of calcium-myofilament interactions with length and force-dependent actin-myosin binding kinetics defined during isovolumic contractions can predict the complex myocardial contractile behavior on ejecting contractions. It is not necessary to introduce length-dependent myofilament calcium affinity for the four-state model to explain contractile behavior on ejecting beats. Prior investigators advanced the concept of explaining whole heart behavior on the basis of the fundamental principles of muscle contraction (10, 11, 17, 26). The present study represents another step toward this goal by offering a comprehensive explanation for load dependence of ventricular performance, thus advancing understanding of the physiology of the intact heart under physiological conditions.

APPENDIX

Biochemical Model of Interactions between Calcium and Myofilaments

This section summarizes the quantitative aspects of implementing the four-state biochemical model of cross-bridge interactions (Fig. 1). Actin-myosin binding is considered to exist in two forms, a weak, nonforce generating bond (A∼M) and a strong, force generating bond (A-M). In diastole, calcium is low and is dissociated from troponin C (Tn) and weak bonds dominate (*state 1*). As intracellular calcium rises and binds with Tn (*state 2*), strong bonds can be generated (*state 3*). Strong bonds can exist in two forms, a more stable form in which calcium is bound to the myofilaments (*state 3*) and a less stable state with no bound calcium (*state 4*) (3, 5). Thus the core model can be described analytically by the following set of simultaneous equations with seven rate constants

$$\frac{d[Tn \cdot A]}{dt} = -K_1[Ca][Tn \cdot A] + K_3[Ca \cdot Tn \cdot A] + K_{d'}[Tn \cdot A\text{-}M]$$

$$\frac{d[M]}{dt} = -K_a[Ca \cdot Tn \cdot A][M] + K_d[Ca \cdot Tn \cdot A\text{-}M] + K_{d'}[Tn \cdot A\text{-}M]$$

$$\frac{d[Ca \cdot Tn \cdot A]}{dt} = K_1[Ca][Tn \cdot A] + K_d[Ca \cdot Tn \cdot A\text{-}M] - (K_3 + K_a[M])[Ca \cdot Tn \cdot A] \quad (A1)$$

$$\frac{d[Ca \cdot Tn \cdot A\text{-}M]}{dt} = K_2[Ca][Tn \cdot A\text{-}M] + K_a[Ca \cdot Tn \cdot A][M] - (K_4 + K_d)[Ca \cdot Tn \cdot A\text{-}M]$$

$$\frac{d[Tn \cdot A\text{-}M]}{dt} = K_4[Ca \cdot Tn \cdot A\text{-}M] - (K_2[Ca] + K_{d'})[Tn \cdot A\text{-}M]$$

Myofilament cooperativity is introduced into the model by assuming that K_1 (calcium binding affinity of the myofilaments) and K_a (actin-myosin binding affinity) varied with the number of strong actin-myosin bonds as detailed previously (3, 25.)

$$K_1(t) = K_{1\alpha}([Ca \cdot Tn \cdot A\text{-}M] + [Tn \cdot A\text{-}M])^{K_{1\gamma}} + K_{1\beta}$$

$$K_a(t) = K_{a\alpha}([Ca \cdot Tn \cdot A\text{-}M] + [Tn \cdot A\text{-}M])^{K_{a\gamma}} + K_{a\beta} \quad (A2)$$

where t is time, $K_{1\alpha}$, $K_{a\alpha}$, $K_{1\beta}$, and $K_{a\beta}$ are adjustable constants, and $K_{1\gamma}$ and $K_{a\gamma}$ are constants set at 0.5 and 2.0, respectively, according to previous empirical analytical studies (3). Other possible means of introducing cooperativity based on K_2, K_3, and K_4 were studied in the past; these failed to yield physiological model behavior and are not discussed further here.

These equations were programmed on a digital computer for numerical solution as described in detail previously (3). The total concentration of actin and myosin were set at 70 and 20 μmol/l, respectively, as indicated in previous studies (3, 5). The driving function for this set of equations was the measured instantaneous calcium concentration. The output of the model was the instantaneous myocardial stress that is assumed to be proportional to the total concentration of strong actin-myosin bonds according to the following equation

$$\sigma(t) = \alpha(\varepsilon)([Ca \cdot Tn \cdot A\text{-}M] + [Tn \cdot A\text{-}M]) \quad (A3)$$

where $\alpha(\varepsilon)$ is proportional to the force generated by a single cross bridge as a function of sarcomere strain (28). We assumed that 0.1 μmol/l of strong bound cross bridge could generate 1 mmHg of muscle stress; thus $\alpha(\varepsilon)$ were defined as

$$\alpha(\varepsilon) = \frac{10\varepsilon - 7}{3} \cdot \frac{1}{0.1} \quad (A4)$$

where $\alpha(\varepsilon)$ is the force per unit cross bridge (mmHg·μmol^{-1}·l^{-1}) (28). Values for the rate constants were optimized to provided optimal agreement between predicted and measured myocardial stress according to the downhill simplex algorithm.

This work was supported by grants from the National Heart, Lung, and Blood Institute (1-R29-HL-51885-01) and the Whitaker Foundation. D. Burkhoff was supported by an Investigatorship Award from the American Heart Association, New York City Affiliate.

REFERENCES

1. **Allen DG and Kentish JC.** The cellular basis of the length-tension relation in cardiac muscle. *J Mol Cell Cardiol* 17: 821–840, 1985.
2. **Allen DG and Kurihara S.** The effects of muscle length on intracellular calcium transients in mammalian cardiac muscle. *J Physiol (Lond)* 327: 79–94, 1982.
3. **Baran D, Ogino K, Stennett R, Schnellbacher M, Zwas D, Morgan JP, and Burkhoff D.** Interrelating of ventricular pressure and intracellular calcium in intact hearts. *Am J Physiol Heart Circ Physiol* 273: H1509–H1522, 1997.
4. **Brandt PW, Colomo F, Piroddi N, Poggesi C, and Tesi C.** Force regulation by Ca^{2+} in skinned single cardiac myocytes of frog. *Biophys J* 74: 1994–2004, 1998.
5. **Burkhoff D.** Explaining load dependence of ventricular contractile properties with a model of excitation-contraction coupling. *J Mol Cell Cardiol* 26: 959–978, 1994.
6. **Burkhoff D, De Tombe PP, and Hunter WC.** Impact of ejection on magnitude and time course of ventricular pressure-generating capacity. *Am J Physiol Heart Circ Physiol* 265: H899–H909, 1993.
7. **Burkhoff D, de Tombe PP, Hunter WC, and Kass DA.** Contractile strength and mechanical efficiency of left ventricle

are enhanced by physiological afterload. *Am J Physiol Heart Circ Physiol* 260: H569–H578, 1991.
8. **Burkhoff D, Yue DT, Franz MR, Hunter WC, Sunagawa K, Maughan WL, and Sagawa K.** Quantitative comparison of the force-interval relationships of the canine right and left ventricles. *Circ Res* 54: 468–473, 1984.
9. **Campbell K.** Rate constant of muscle force redevelopment reflects cooperative activation as well as cross-bridge kinetics. *Biophys J* 72: 254–262, 1997.
10. **Campbell KB, Shroff SG, and Kirkpatrick RD.** Short-timescale left ventricular systolic dynamics. Evidence for a common mechanism in both left ventricular chamber and heart muscle mechanics. *Circ Res* 68: 1532–1548, 1991.
11. **Campbell KB, Taheri H, Kirkpatrick RD, Burton T, and Hunter WC.** Similarities between dynamic elastance of left ventricular chamber and papillary muscle of rabbit heart. *Am J Physiol Heart Circ Physiol* 264: H1926–H1941, 1993.
12. **Delhaas T, Arts T, Bovendeerd PH, Prinzen FW, and Reneman RS.** Subepicardial fiber strain and stress as related to left ventricular pressure and volume. *Am J Physiol Heart Circ Physiol* 264: H1548–H1559, 1993.
13. **Hill AV.** Heat of shortening and the dynamic constants of muscle. *Proc R Soc Lond B Biol Sci* 126: 136–195, 1938.
14. **Housmans PR, Lee NK, and Blinks JR.** Active shortening retards the decline of the intracellular calcium transient in mammalian heart muscle. *Science* 221: 159–161, 1983.
15. **Hunter WC.** End-systolic pressure as a balance between opposing effects of ejection. *Circ Res* 64: 265–275, 1989.
16. **Hunter WC and Baan J.** The role of wall thickness in the relation between sarcomere dynamics and ventricular dynamics. In: *Cardiac Dynamics*, edited by Baan J, Arntzenius AC, and Yellin EL. The Hague, The Netherlands: Nijhoff, 1980, p. 123–134.
17. **Izakov V, Katsnelson LB, Blyakhman FA, Markhasin VS, and Shklyar TF.** Cooperative effects due to calcium binding by troponin and their consequences for contraction and relaxation of cardiac muscle under various conditions of mechanical loading. *Circ Res* 69: 1171–1184, 1991.
18. **Janssen PM and de Tombe PP.** Uncontrolled sarcomere shortening increases intracellular Ca^{2+} transient in rat cardiac trabeculae. *Am J Physiol Heart Circ Physiol* 272: H1892–H1897, 1997.
19. **Kentish JC and Wrzosek A.** Changes in force and cytosolic Ca^{2+} concentration after length changes in isolated rat ventricular trabeculae. *J Physiol (Lond)* 506: 431–444, 1998.
20. **Kihara Y, Grossman W, and Morgan JP.** Direct measurement of changes in intracellular calcium transients during hypoxia, ischemia, and reperfusion of the intact mammalian heart. *Circ Res* 65: 1029–1044, 1989.
21. **Kurihara S and Komukai K.** Tension-dependent changes of the intracellular Ca^{2+} transients in ferret ventricular muscles. *J Physiol (Lond)* 489: 617–625, 1995.
22. **Landesberg A and Sideman S.** Mechanical regulation of cardiac muscle by coupling calcium kinetics with cross-bridge cycling: a dynamic model. *Am J Physiol Heart Circ Physiol* 267: H779–H795, 1994.
23. **McDonald KS, Wolff MR, and Moss RL.** Sarcomere length dependence of the rate of tension redevelopment and submaximal tension in rat and rabbit skinned skeletal muscle fibres. *J Physiol (Lond)* 501: 607–621, 1997.
24. **Metzger JM and Moss RL.** Calcium-sensitive cross-bridge transitions in mammalian fast and slow skeletal muscle fibers. *Science* 247: 1088–1090, 1990.
25. **Nagashima H and Asakura S.** Studies on co-operative properties of tropomyosin-actin and tropomyosin-troponin-actin complexes by the use of *N*-ethylmaleimide-treated and untreated species of myosin subfragment 1. *J Mol Biol* 155: 409–428, 1982.
26. **Shroff SG, Campbell KB, and Kirkpatrick RD.** Short timescale LV systolic dynamics: pressure vs. volume clamps and effect of activation. *Am J Physiol Heart Circ Physiol* 264: H946–H959, 1993.
27. **Shroff SG, Janicki JS, and Weber KT.** Evidence and quantitation of left ventricular systolic resistance. *Am J Physiol Heart Circ Physiol* 249: H358–H370, 1985.
28. **Stennett R, Ogino K, Morgan JP, and Burkhoff D.** Length-dependent activation in intact ferret hearts: study of steady-state Ca^{2+}-stress-strain interrelations. *Am J Physiol Heart Circ Physiol* 270: H1940–H1950, 1996.
29. **Suga H, Sagawa K, and Shoukas AA.** Load independence of the instantaneous pressure-volume ratio of the canine left ventricle and effects of epinephrine and heart rate on the ratio. *Circ Res* 32: 314–322, 1973.
30. **Sunagawa K, Burkhoff D, Lim KO, and Sagawa K.** Impedance loading servo pump system for excised canine ventricle. *Am J Physiol Heart Circ Physiol* 243: H346–H350, 1982.
31. **Sunagawa K, Lim KO, Burkhoff D, and Sagawa K.** Microprocessor control of a ventricular volume servo-pump. *Ann Biomed Eng* 10: 145–159, 1982.
32. **Todaka K, Ogino K, Gu A, and Burkhoff D.** Effect of ventricular stretch on contractile strength, calcium transient, and cAMP in intact canine hearts. *Am J Physiol Heart Circ Physiol* 274: H990–H1000, 1998.